

Crucial steps for robust first quiescent region truncated partial Euler Product based approximations of closely spaced Riemann Zeta function non-trivial zeroes.

John Martin

May 20, 2025

Executive summary

First quiescent region $N_1 = \sqrt{\frac{t}{2\pi}}$ truncated partial Euler Product based approximations of the Riemann Siegel Z function can be made robust by the following steps (i) spectral filtering and phase conjugate reflection of the partial Euler Product fourier transform, (ii) setting the imaginary parts of $\text{fft}[1]$ and (for n real) $\text{fft}[\lceil \frac{n}{2} \rceil + 1]$ equal to zero, (iii) using the primes over $N_1 + \Delta$ rather than N_1 and (iv) averaging the results of inverse fourier transforms of the partial Euler product based Riemann Siegel Z function (of different spectrum widths). These steps reduce the impact of spectral leakage from high frequency components present in the partial Euler Product (but not contained in the Riemann Zeta function) resulting in agreement with the Riemann Zeta function to 6+ decimal places which is required for inspecting closely spaced non-trivial zeroes.

Introduction

The Riemann Zeta function is defined [1-3], in the complex plane by the integral

$$\zeta(s) = \frac{\prod(-s)}{2\pi i} \int_{C_{\epsilon,\delta}} \frac{(-x)^s}{(e^x - 1)x} dx \quad (1)$$

where $s \in \mathbb{C}$ and $C_{\epsilon,\delta}$ is the contour about the imaginary poles.

The Riemann Zeta function has been shown to obey the functional equation [1-4]

$$\zeta(s) = \chi(s)\zeta(1-s) \quad (2)$$

$$= 2^s \pi^{s-1} \sin\left(\frac{\pi s}{2}\right) \Gamma(1-s) \zeta(1-s) \quad (3)$$

$$= e^{-2\theta(s)} \zeta(1-s) \quad (4)$$

For $\Re(s) > 1$, the infinite Euler Product of the primes absolutely converges to the infinite Riemann Zeta Dirichlet Series sum [1,3]

$$\zeta(s) = \sum_{k=1}^{\infty} \frac{1}{k^s} = \prod_{\rho=2}^{\infty} \frac{1}{(1 - 1/\rho^s)} \quad \text{for } \Re(s) > 1 \quad (5)$$

Of interest to this paper is the Riemann-Siegel Z function of the Riemann Zeta function

$$Z_{\zeta}(0.5 + I \cdot t) = e^{I \cdot \theta(t)} \zeta(0.5 + I \cdot t) \quad (6)$$

and how the partial Euler Product version of Riemann-Siegel Z function using truncation at the first quiescent region $N_1 = \sqrt{\frac{t}{2\pi}}$

$$Z_{\zeta}(0.5 + I \cdot t) \approx e^{I \cdot \theta(t)} \left(\prod_{p=2}^{p \leq \lfloor \sqrt{\frac{t}{2\pi}} \rfloor = N_1} \frac{1}{(1 - \frac{1}{p^{(0.5+I \cdot t)}})} + \chi(0.5 + I \cdot t) \cdot \prod_{p=2}^{p \leq \lfloor \sqrt{\frac{t}{2\pi}} \rfloor = N_1} \frac{1}{(1 - \frac{1}{p^{(1-(0.5+I \cdot t))}})} \right) \quad (7)$$

may be improved particularly near closely spaced Riemann Zeta function non-trivial zeroes.

In this paper, the spectral filtering approach of [5] is followed concentrating on the Riemann-Siegel Z function calculation because of its higher symmetry with respect to fourier transform components. In [5] it was identified for $N_1 = \sqrt{\frac{t}{2\pi}}$ truncation of the partial Euler Product the first $\prod_{p=2}^{p \leq \lfloor \sqrt{\frac{t}{2\pi}} \rfloor} \frac{1}{(1 - \frac{1}{p^{(0.5+I \cdot t)}})}$ and second $\chi(0.5 + I \cdot t) \cdot \prod_{p=2}^{p \leq \lfloor \sqrt{\frac{t}{2\pi}} \rfloor} \frac{1}{(1 - \frac{1}{p^{(1-(0.5+I \cdot t))}})}$ components of the RHS of equation (7), respectively contribute different angular frequency components of the fourier transform. The spectral filtering of the fourier transform attempts to (efficiently) throw away nuisance angular frequency components in the above components that are not present in the proper Riemann Zeta and Riemann-Siegel Z functions.

To test the performance of the partial Euler Product version of Riemann-Siegel Z function using truncation at the first quiescent region for closely spaced Riemann Zeta non-trivial zeroes the extremely narrow pair of zeroes at 388858886.0022851... and 388858886.0023936... [6,7] is at the centre of the critical line interval investigated ($t=388858886+(-750,750)$).

The paper illustrates four crucial steps that enable robust approximations (to 6+ decimal places) in the Riemann-Siegel Z function via the partial Euler Product using N_1 (first quiescent region) hence allowing inspection of closely spaced Riemann Zeta function non-trivial zeroes.

1. using phase conjugate reflection (about the DC fourier component) of the most accurate fourier transform components of $e^{I \cdot \theta(t)} \prod_{p=2}^{p \leq \lfloor \sqrt{\frac{t}{2\pi}} \rfloor} \frac{1}{(1 - \frac{1}{p^{(0.5+I \cdot t)}})}$ or $e^{I \cdot \theta(t)} \chi(0.5 + I \cdot t) \cdot \prod_{p=2}^{p \leq \lfloor \sqrt{\frac{t}{2\pi}} \rfloor} \frac{1}{(1 - \frac{1}{p^{(1-(0.5+I \cdot t))}})}$ to derive a zeroth order approximation of $e^{I \cdot \theta(t)} \zeta(0.5 + I \cdot t)$.
2. using truncation at $N_1 + \Delta$ (rather than N_1) to reduce the approximation errors in Riemann-Siegel Z function approximation based on the partial Euler Product
3. setting the imaginary(DC fourier component) = 0 and for n real imaginary($\text{fft}[\lfloor \frac{n}{2} \rfloor + 1]$) = 0 to enhance the symmetry/continuity of the approximate fourier transform to improve approximation accuracy since the function to be predicted the Riemann-Siegel Z function is known to be strictly real
4. execute and average fourier analyses of differing lengths as the fourier transform component errors in this partial Euler Product Riemann-Siegel Z function approximation appears to vary in random manner across the different length transforms.

The final step of averaging across many fourier transforms (of differing length) adds to the computational cost but it is a minor cost component (for large t values) since each fourier analysis is re-examining the single Riemann_Siegel Z function spectrum obtained efficiently by the partial Euler Product calculation.

Comparing the fourier transform spectra of the Riemann Zeta function and first quiescent region based partial Euler Product calculations

Using spectral filtering and phase conjugate reflection to achieve zeroth order approximation for all fourier components

Figure 1 illustrates the absolute value of the fourier transform of (i) the Riemann-Siegel Z function of the Riemann Zeta function

$$e^{\theta(t)}\zeta(0.5 + I \cdot t) \quad (8)$$

(shown in the middle row repeated) and (ii) the two components of the Riemann-Siegel Z function of the partial Euler Product truncated at the first quiescent region

first component (lefthand panel top row);

$$e^{I \cdot \theta(t)} \prod_{p=2}^{p \leq \lfloor \sqrt{\frac{t}{2\pi}} \rfloor} \frac{1}{(1 - \frac{1}{p^{(0.5+I \cdot t)}})} \quad (9)$$

second component (lefthand panel bottom row);

$$e^{I \cdot \theta(t)} \chi(0.5 + I \cdot t) \cdot \prod_{p=2}^{p \leq \lfloor \sqrt{\frac{t}{2\pi}} \rfloor} \frac{1}{(1 - \frac{1}{p^{(1-(0.5+I \cdot t))}})} \quad (10)$$

are compared over the interval $t=38885886+(-750,750)$ respectively, on the critical line $\Re(s) = 0.5$.

Most importantly, in the top and bottom rows are phase conjugate reflections of the useful positive (negative) angular frequency halves of the first (second) components respectively of the Riemann-Siegel Z function of the partial Euler Product truncated at the first quiescent region about the DC fourier component where the reflected half is highlighted in green.

To produce figure 1, firstly the $e^{\theta(t)}\zeta(0.5 + I \cdot t)$, $e^{I \cdot \theta(t)} \prod_{p=2}^{p \leq \lfloor \sqrt{\frac{t}{2\pi}} \rfloor} \frac{1}{(1 - \frac{1}{p^{(0.5+I \cdot t)}})}$ and $e^{I \cdot \theta(t)} \chi(0.5 + I \cdot t) \cdot \prod_{p=2}^{p \leq \lfloor \sqrt{\frac{t}{2\pi}} \rfloor} \frac{1}{(1 - \frac{1}{p^{(1-(0.5+I \cdot t))}})}$ functions were calculated for a grid of points for $\Re(s) = 0.5$ value ($t = (38885886 - 750, 38885886 + 750)$), with a spacing 0.01 giving a waveform sample of 149999 points) and stored to file using the pari-gp language [8] and secondly the fourier transform calculations and graphs were derived using the R language [9] and Rstudio IDE [10].

The reference Riemann-Siegel Z function was calculated using the Riemann-Siegel formula via 128 point tapered Dirichlet series approximation (which has about 28 decimal place precision at $s = 0.5 + I \cdot 38885886$)

$$\begin{aligned} e^{I \cdot \theta(0.5+I \cdot t)} \zeta_{RS \text{ tapered}}(0.5 + I \cdot t) &= e^{I \cdot \theta(0.5+I \cdot t)} \left[\sum_{n=1}^{(\lfloor \sqrt{\frac{t}{2\pi}} \rfloor - q)} \frac{1}{n^{(0.5+I \cdot t)}} + \sum_{i=(-q+1)}^q \frac{\frac{1}{2^{2q}} \left(2^{2q} - \sum_{k=0}^{i+q-1} \binom{2q}{2q-k} \right)}{(\lfloor \sqrt{\frac{t}{2\pi}} \rfloor + i)^{(0.5+I \cdot t)}} \right] \\ &+ \chi(0.5 + I \cdot t) \cdot \left(\sum_{n=1}^{(\lfloor \sqrt{\frac{t}{2\pi}} \rfloor - q)} \frac{1}{n^{(1-(0.5+I \cdot t))}} + \sum_{i=(-q+1)}^q \frac{\frac{1}{2^{2q}} \left(2^{2q} - \sum_{k=0}^{i+q-1} \binom{2q}{2q-k} \right)}{(\lfloor \sqrt{\frac{t}{2\pi}} \rfloor + i)^{(1-(0.5+I \cdot t))}} \right) \end{aligned} \quad \text{as } t \rightarrow \infty \quad (11)$$

Since the input data of a Riemann-Siegel Z function on the critical line is real valued, the fourier transform spectrum of a Riemann-Siegel Z function is two sided. For convenience in figure 1,

1. the fast fourier transform (fft) output vector is wrapped around so that the informative non-zero fft components appear next to the DC fourier component axis as positive and negative frequency components.
2. the x-axis is scaled in units of angular frequency (radians per second).

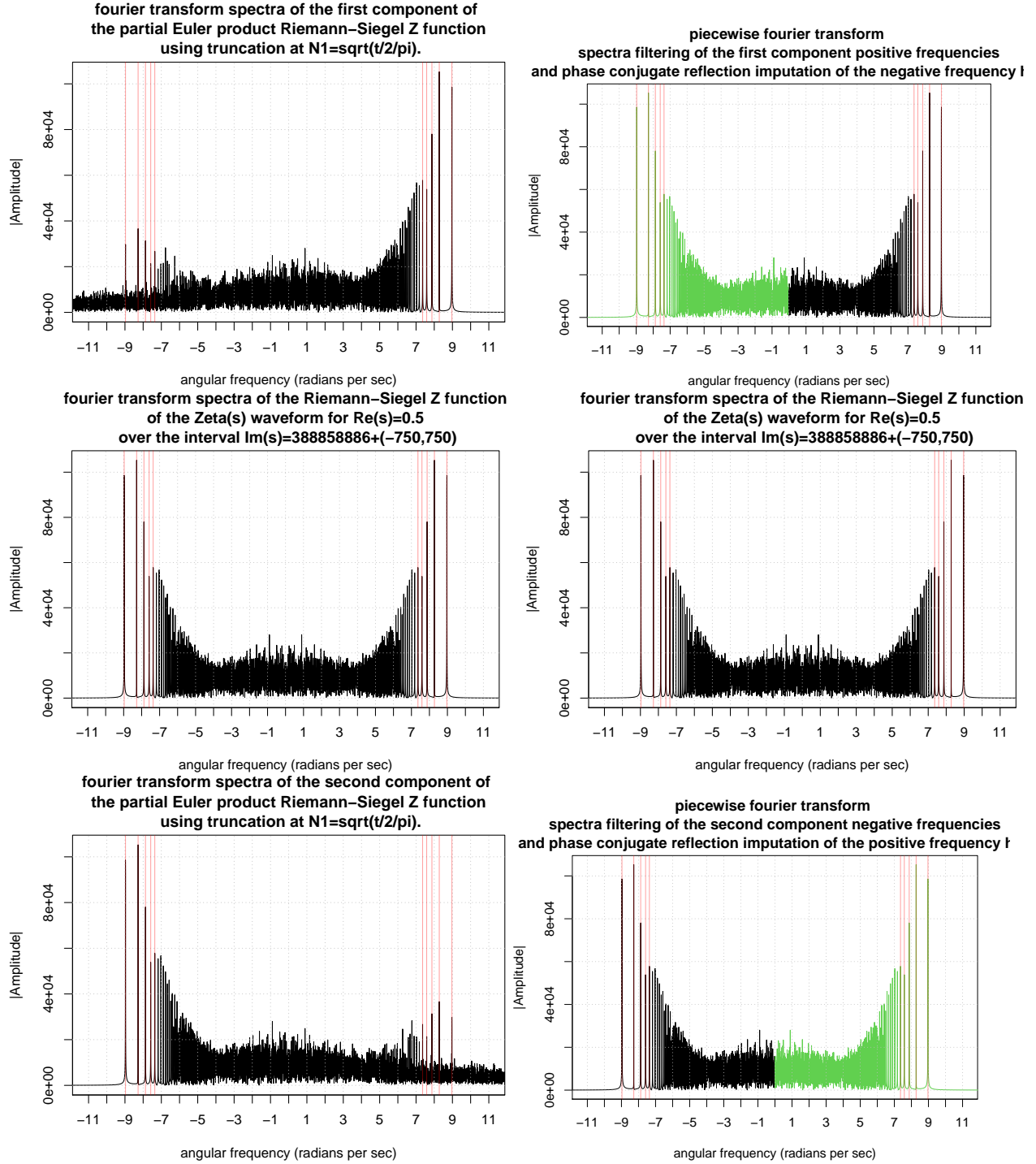


Figure 1: A comparison of the fourier transforms of the Riemann-Siegel Z functions of the Riemann Zeta function and partial Euler Product (using truncation at $N_1 = \sqrt{\frac{t}{2\pi}}$ in the complex plane at $\sigma = 0.5$ for the interval $t=388858886+(-750,750)$). The positions of the frequency features indicated by red are successfully captured as a function of t by the expressions postulated in the paper. To help use the partial Euler Product as an approximation of the Riemann-Siegel Z function phase conjugate reflection of the (accurate part of) partial Euler Product fourier transform about angular frequency = zero as shown in green is a strong zeroth order improvement.

As indicated by the red vertical lines there are broad spectral features which can be successfully captured by the assignment of the pair of bounds $\pm \frac{1}{2}(\log(UB/\pi/2), \log(LB/\pi/2))$, $\pm \frac{1}{2}(\log(UB/\pi/2/2^2), \log(LB/\pi/2/2^2))$, $\pm \frac{1}{2}(\log(UB/\pi/2/3^2), \log(LB/\pi/2/3^2))$ etc where $UB=388858886+750, LB=388858886-750$ corresponding to the range of t values collected in the spectrum. These spectral features can be obtained from the leading terms of the dirichlet series and the $\theta(0.5 + I \cdot t)$ function

Using the well known dirichlet series version of equation (7) [1-4]

$$Z_\zeta(0.5 + I \cdot t) \approx e^{I \cdot \theta(t)} \left(\sum_{n=1}^{n \leq \lfloor \sqrt{\frac{t}{2\pi}} \rfloor = N_1} \frac{1}{n^{(0.5+I \cdot t)}} + \chi(0.5 + I \cdot t) \cdot \sum_{n=1}^{n \leq \lfloor \sqrt{\frac{t}{2\pi}} \rfloor = N_1} \frac{1}{n^{(1-(0.5+I \cdot t))}} \right) \quad (12)$$

and considering only the leading terms and $n=1,2,3,4,\dots$

for the first summation term there are the components

$$e^{I \cdot \theta(t)} \cdot \frac{1}{n^{(0.5+I \cdot t)}} = \frac{1}{n^{0.5}} \cdot e^{I \cdot (\theta(t) - t \log(n))} \quad (13)$$

$$= \frac{1}{n^{0.5}} \cdot e^{I \cdot (\frac{1}{2} t \cdot \log(\frac{t}{2\pi}) + \dots - t \log(n))} \quad (14)$$

$$= \frac{1}{n^{0.5}} \cdot e^{I \cdot (t \cdot \log(\sqrt{\frac{t}{2\pi}}) + \dots - t \log(n))} \quad (15)$$

$$= \frac{1}{n^{0.5}} \cdot e^{I \cdot (t \cdot \log(\sqrt{\frac{t}{2\pi} \cdot \frac{1}{n}}) + \dots)} \quad (16)$$

$$= \frac{1}{n^{0.5}} \cdot e^{I \cdot (t \cdot \log(\sqrt{\frac{t}{n^2 \cdot 2\pi}}) + \dots)} \quad (17)$$

$$= \frac{1}{n^{0.5}} \cdot e^{I \cdot (\frac{1}{2} t \cdot \log(\frac{t}{n^2 \cdot 2\pi}) + \dots)} = \frac{1}{n^{0.5}} \cdot e^{I \cdot \omega_n t} \quad (18)$$

likewise for the second summation term there are the components

$$e^{I \cdot \theta(t)} \cdot e^{-2 \cdot I \cdot \theta(t)} \cdot \frac{1}{n^{(1-(0.5+I \cdot t))}} = \frac{1}{n^{0.5}} \cdot e^{I \cdot (-\theta(t) + t \log(n))} \quad (19)$$

$$= \frac{1}{n^{0.5}} \cdot e^{I \cdot (-\frac{1}{2} t \cdot \log(\frac{t}{2\pi}) + \dots + t \log(n))} \quad (20)$$

$$= \frac{1}{n^{0.5}} \cdot e^{I \cdot (-t \cdot \log(\sqrt{\frac{t}{2\pi}}) + \dots + t \log(n))} \quad (21)$$

$$= \frac{1}{n^{0.5}} \cdot e^{I \cdot (-t \cdot \log(\sqrt{\frac{t}{2\pi} \cdot \frac{1}{n}}) + \dots)} \quad (22)$$

$$= \frac{1}{n^{0.5}} \cdot e^{I \cdot (-t \cdot \log(\sqrt{\frac{t}{n^2 \cdot 2\pi}}) + \dots)} \quad (23)$$

$$= \frac{1}{n^{0.5}} \cdot e^{I \cdot (-\frac{1}{2} t \cdot \log(\frac{t}{n^2 \cdot 2\pi}) + \dots)} = \frac{1}{n^{0.5}} \cdot e^{-I \cdot \omega_n t} \quad (24)$$

yielding the leading values of the fourier transform component angular frequencies

$$\omega_n \approx \pm \frac{1}{2} \log\left(\frac{t}{n^2 \cdot 2\pi}\right) \text{ where } n=1,2,3,\dots, \lfloor \sqrt{\frac{t}{2\pi}} \rfloor$$

So the positive (negative) angular frequencies of the first (second) component of the partial Euler Product truncated at N_1 of the Riemann Siegel Z function can be clearly seen to be a reasonable zeroth order approximations of the fourier transform of the true Riemann Siegel Z function and using a phase conjugate reflection of these good fourier transform parts of the first (second) component of the partial Euler Product truncated at N_1 of the Riemann Siegel Z function provides zeroth order replications of both the peaks at

low frequencies and the featureless shoulders at high positive/negative frequencies. In contrast, in [5] the shoulder region of the fourier transform of the Riemann Zeta function approximation was simply imputed with zeroes which limits the precision achievable by that earlier approach.

Assessing the dependence of the errors in real and imaginary parts of the zeroth order fourier transform approximation on the truncation length of the finite product of primes

Figure 2 illustrates the elementwise difference between the real and imaginary parts respectively of the (two) zeroth order approximation Riemann-Siegel Z function fourier transforms and the true Riemann-Siegel Z function fourier transform over the interval $t=38885886+(-750,750)$, on the critical line $\Re(s) = 0.5$ for three different truncation lengths of the finite product of primes $N_1, N_1 + 2000, 3 \cdot N_1$.

It can be seen that

1. comparing the lefthand column to the righthand column graphs the errors for the two possible spectral filtering and phase conjugate reflection approximation (biased on the first or second component of equation (7)) are essentially the same consistent with the higher symmetry of the Riemann-Siegel Z function compared to the Riemann Zeta function
2. comparing the rows increasing the truncation length beyond N_1 helps reduce the elementwise errors in the fourier components
3. that largest error occurs for the DC fourier component

Fine tuning the symmetry and/or continuity of imaginary part of the zeroth order fourier transform approximation for the DC, $\text{ceiling}(n/2)$ and $(\text{ceiling}(n/2)+1)$ fourier components

In finer detail, the true discrete Riemann-Siegel Z function has a zero imaginary part at

- (i) the DC fourier component (occurring numerically as `fft_zeta_Zfn[1]`)

example

```
fft_zeta_Zfn[c(n,1,2)]
[1] -2149.371-45.732i -1826.913+ 0.000i -2149.371+45.732i
```

- (ii) when circularly joining the positive and negative frequency ends together in the frequency domain (occurring numerically as between the fourier components `fft_zeta_Zfn[ceiling(n/2)]` and `fft_zeta_Zfn[ceiling(n/2)+1]`) the imaginary component has values close to zero during sign change

example

```
fft_zeta_Zfn[ceiling(n/2)+c(-1,0,1,2,3)]
[1] -0.8394496+0.0000260i -0.8394496+0.0000087i -0.8394496-0.0000087i -0.8394496-0.0000260i
[5] -0.8394496-0.0000434i
```

Therefore to enhance the spectral filtering and phase conjugate reflection approximation of the partial Euler product

- the non-zero imaginary part of the DC component of the approximation fourier transform (shown as a black circle in figure 2) is imputed to zero to match the true discrete fourier transform imaginary part DC component of Riemann-Siegel Z function behavior
- for n real, the imaginary part of the $(\text{ceiling}(n/2)+1)$ component of the approximation fourier transform is imputed to zero to more closely resemble the true discrete fourier transform imaginary part of Riemann-Siegel Z function behavior (since it clearly very strongly sets the imaginary part of the inverse fourier transform to zero i.e., producing a real function)

- material added: For discrete fourier transforms of real waveforms [11] it is already known that the discrete fourier transform must (i) have phase conjugate symmetry and $\text{imaginary}(\text{fft}[1])=0$ and (ii) for even sample sizes (i.e., n even) $\text{imaginary}(\text{fft}[\text{ceiling}(n/2)+1])=0$. So applying these constraints to the partial Euler Product approximation of the Riemann-Siegel Z function is logical in order to achieve a purely real predicted function. The difference in this paper to applying such already known DFT properties [11] is that averaging of fourier analysis of different sample sizes is also executed to suppress spectral leakage/aliasing.

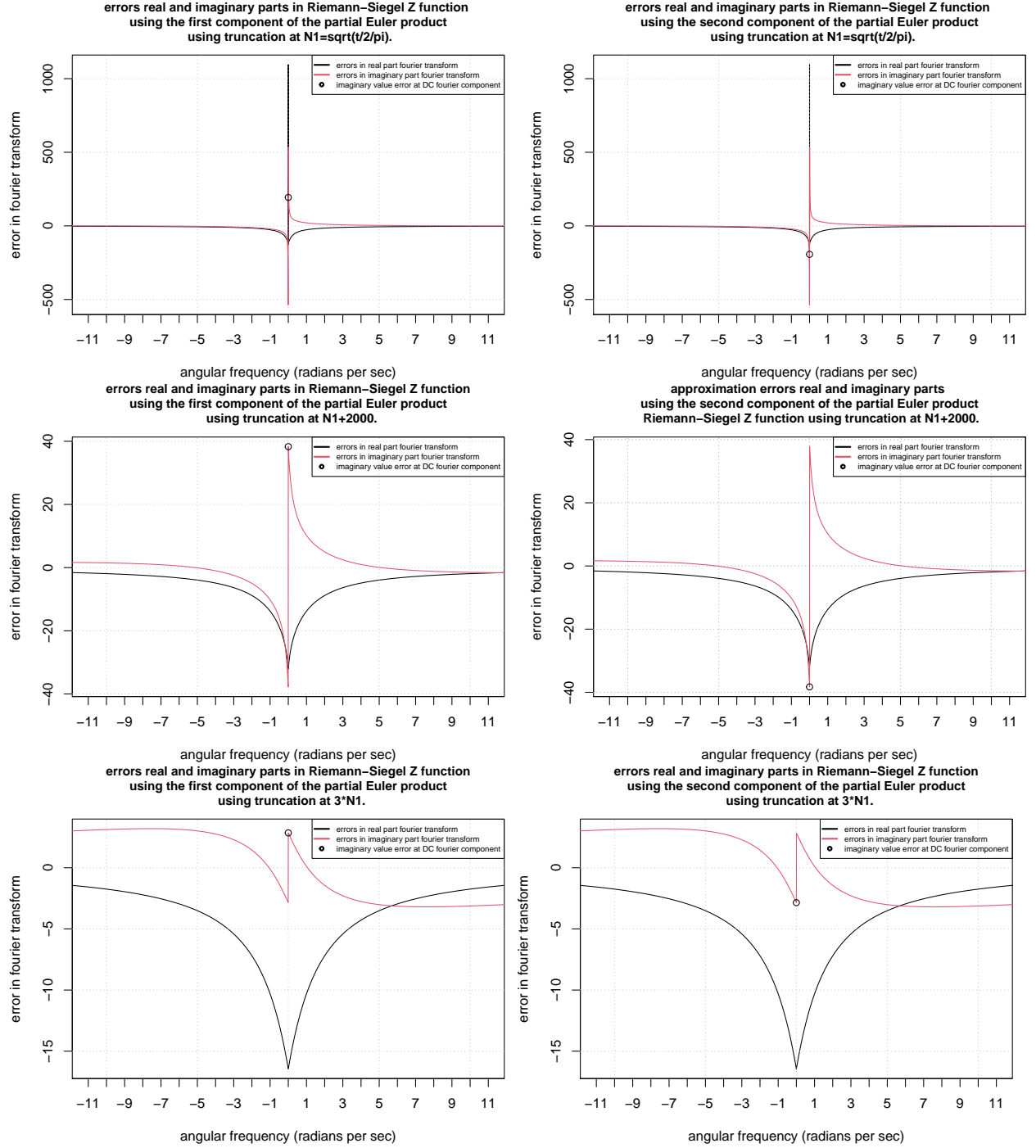


Figure 2: A comparison of the elementwise difference in the fourier transforms of the Riemann-Siegel Z functions of the Riemann Zeta function and partial Euler Product using three truncation lengths (top row $N_1 = \sqrt{\frac{t}{2\pi}}$, middle row $N_1 + 2000$, bottom row $3N_1$) in the complex plane at $\sigma = 0.5$ for the interval $t=388858886+(-750,750)$..

Using averaging of (fourier transforms and their) inverse fourier transforms of different lengths to cancel out partial Euler product fourier transform approximation errors

On inspection of varying the length of the fourier transform of the partial Euler product approximation of the Riemann-Siegel Z function it was observed that the approximation errors in the fourier components varied sign. Thus it became important to investigate whether the fourier transform errors in the partial Euler product approximation could be cancelled by averaging over the results of fourier transforms (and inverse fourier transforms) of different lengths.

As the results for example A indicate (i) this averaging step and (ii) partial Euler Product truncation $> N_1$ can both be very beneficial to the approximation accuracy.

As the results for example B indicate using a wider input spectrum for analysis can be beneficial to the approximation accuracy (since truncation $\gg N_1$ would greatly increase the partial Euler Product calculation time).

example A; reference value - Riemann-Siegel Z function value at $s = 0.5 + I \cdot 388858886$

using fourier transform of first component of partial Euler product approximation of Riemann-Siegel Z function applying spectral filtering and phase conjugate reflection about DC component setting imaginary part of DC fourier component to zero for n real setting only the imaginary part of $(\text{ceiling}(n/2)+1)$ fourier component to zero in partial Euler product approximation

pari-gp [8] calculation using 128 tapered Dirichlet series truncation at N_1

```
dirichRS_S_sum128(0.5+I*388858886)*exp(I*vtheta(388858886))
```

```
time = 116 ms.
```

```
%31 = 0.00041148914820069374095342320372253831362 + 9.442756329679734991 E-33*I
```

approximation 1 - based on partial Euler Product truncation at N_1

using spectrum collected in the interval $t=388858886+(-750,750)$

maximum available sample $n=149999$

below is the inverse fourier transform result for the Riemann-Siegel Z function at $s = 0.5 + I \cdot 388858886$ under 1000 iterations of fourier transforms of different sample lengths

```
[1] "index; single run estimate; sample length; cumulative average"
[1] "1 8.49768103287636e-03+5.4e-16i 129920 8.49768103287636e-03+5.4e-16i"
[1] "2 8.49794082199887e-03-3.8e-16i 129940 8.49781092743761e-03+8e-17i"
[1] "3 8.49823675472306e-03-2.2e-16i 129960 8.4979528698661e-03-2e-17i"
[1] "4 8.49858167929387e-03+9e-17i 129980 8.49811007222304e-03+7e-18i"
[1] "5 8.49895691678528e-03-1.11e-15i 130000 8.49827944113549e-03-2.2e-16i"
[1] "6 8.49932606353117e-03+7.3e-16i 130020 8.49845387820143e-03-6e-17i"
[1] "7 8.49965765251919e-03-1.1e-16i 130040 8.49862584596111e-03-7e-17i"
[1] "8 8.49994037947753e-03+6.5e-16i 130060 8.49879016265066e-03+2e-17i"
[1] "9 8.5001887231925e-03-3e-17i 130080 8.49894555826643e-03+2e-17i"
[1] "10 8.50043180720463e-03-7.27e-15i 130100 8.49909418316025e-03-7.1e-16i"
...
[1] "991 8.61783159103806e-03-4.9e-16i 149720 8.57243955748697e-03-8e-18i"
[1] "992 8.61784276533639e-03-1e-16i 149740 8.57248532684972e-03-8e-18i"
[1] "993 8.61786488285779e-03+9e-17i 149760 8.5725310263019e-03-8e-18i"
[1] "994 8.61788466528794e-03-3.2e-16i 149780 8.5725766537053e-03-8e-18i"
[1] "995 8.61789676627772e-03+2.2e-16i 149800 8.57262220155713e-03-8e-18i"
[1] "996 8.61790483276872e-03+3.1e-16i 149820 8.5726676660463e-03-8e-18i"
[1] "997 8.61790957968082e-03-5.1e-16i 149840 8.57271304409408e-03-8e-18i"
[1] "998 8.61790829377404e-03+5.3e-16i 149860 8.5727583299154e-03-7e-18i"
[1] "999 8.61789770457076e-03+1.2e-16i 149880 8.57280351447462e-03-7e-18i"
[1] "1000 8.61787530627357e-03+4.76e-15i 149900 0.00857284858626642-0i"
```

The partial Euler Product based estimate after averaging above using truncation at N_1 $Z(0.5+I*388858886) \approx 0.00857284858626642 - 0i$ clearly has a bias with respect to the known Riemann-Siegel Z function value $Z(0.5 + I * 388858886) = 0.00041148914820069374095342320372253831362 + 9.442756329679734991E - 33 * I$

approximation 2 - based on partial Euler Product truncation at $N_1 + 2000$

maximum available sample $n=149999$

below is the inverse fourier transform result for the Riemann-Siegel Z function at $s = 0.5 + I \cdot 388858886$ under 1000 iterations of fourier transforms of different sample lengths

```
[1] "index; single run estimate; sample length; cumulative average"
[1] "1 4.09371524606039e-04+8.89e-16i 129920 4.09371524606039e-04+8.89e-16i"
[1] "2 4.0966590672624e-04-1.289e-15i 129940 4.0951871566614e-04-2e-16i"
[1] "3 4.09992297593216e-04+1.022e-15i 129960 4.09676576308499e-04+2.07e-16i"
[1] "4 4.10362501154867e-04-7.58e-16i 129980 4.09848057520091e-04-3.4e-17i"
[1] "5 4.10759435479458e-04-2.3e-16i 130000 4.10030333111964e-04-7.3e-17i"
[1] "6 4.1115072565886e-04+1.208e-15i 130020 4.10217065203113e-04+1.4e-16i"
[1] "7 4.11507348200488e-04-7e-18i 130040 4.10401391345596e-04+1.19e-16i"
[1] "8 4.11818369350253e-04+3.8e-17i 130060 4.10578513596178e-04+1.09e-16i"
[1] "9 4.12097675482704e-04+8e-18i 130080 4.10747309361347e-04+9.8e-17i"
[1] "10 4.12373614171234e-04+9.42e-16i 130100 4.10909939842336e-04+1.82e-16i"
...
[1] "991 4.11435856017834e-04+9.79e-16i 149720 4.11945683089485e-04+2.9e-17i"
[1] "992 4.11387205863618e-04+3.06e-16i 149740 4.1194512010841e-04+3e-17i"
[1] "993 4.11347470088248e-04-3e-17i 149760 4.11944518245349e-04+3e-17i"
[1] "994 4.11303099672093e-04+3.56e-16i 149780 4.11943872955034e-04+3e-17i"
[1] "995 4.11250699815255e-04+4.1e-16i 149800 4.11943176298612e-04+3e-17i"
[1] "996 4.11196085340993e-04-4.09e-16i 149820 4.11942426207289e-04+3e-17i"
[1] "997 4.1113972651385e-04+3.28e-15i 149840 4.1194162109225e-04+3.3e-17i"
[1] "998 4.11078136352287e-04+5.9e-17i 149860 4.1194075587708e-04+3.3e-17i"
[1] "999 4.11007692404555e-04+4.42e-16i 149880 4.1193982187961e-04+3.4e-17i"
[1] "1000 4.10925599788654e-04+2.49e-16i 149900 4.11938807657519e-04+3.4e-17i"
```

The partial Euler Product based estimate after averaging above using truncation at $N_1 + 2000$ $Z(0.5 + I * 388858886) \approx 4.11938807657519e - 04 + 3.4e - 17i$ agrees to 6 decimal places with respect to the known Riemann-Siegel Z function value $Z(0.5 + I * 388858886) = 0.00041148914820069374095342320372253831362 + 9.442756329679734991E - 33 * I$

approximation 3 - based on partial Euler Product truncation at $3N_1$

maximum available sample $n=149999$

below is the inverse fourier transform result for the Riemann-Siegel Z function at $s = 0.5 + I \cdot 388858886$ under 1000 iterations of fourier transforms of different sample lengths

```
[1] "1 4.11547109231009e-04-9.8e-17i 129920 4.11547109231009e-04-9.8e-17i"
[1] "2 4.11548431336232e-04-9.04e-16i 129940 4.1154777028362e-04-5.01e-16i"
[1] "3 4.11569975803885e-04-3.6e-17i 129960 4.11555172123709e-04-3.46e-16i"
[1] "4 4.11615652508731e-04+4.9e-17i 129980 4.11570292219964e-04-2.47e-16i"
[1] "5 4.11659762034049e-04+2.26e-16i 130000 4.11588186182781e-04-1.53e-16i"
[1] "6 4.11679701140506e-04-5.16e-16i 130020 4.11603438675735e-04-2.13e-16i"
[1] "7 4.11668777573243e-04+1.04e-16i 130040 4.11612772803951e-04-1.68e-16i"
[1] "8 4.11624207422545e-04+4.66e-16i 130060 4.11614202131275e-04-8.9e-17i"
[1] "9 4.11556357393006e-04+6.22e-16i 130080 4.11607774938134e-04-1e-17i"
[1] "10 4.11488764037412e-04-6.777e-15i 130100 4.11595873848062e-04-6.86e-16i"
[1] "11 4.11438769355671e-04+4.25e-16i 130120 4.11581591621481e-04-5.85e-16i"
...
[1] "991 4.11437823607544e-04+7.22e-16i 149720 4.11487663521972e-04-3.7e-17i"
[1] "992 4.11449978267239e-04-1.7e-17i 149740 4.11487625532804e-04-3.7e-17i"
[1] "993 4.11473777848688e-04+9.1e-17i 149760 4.11487611587503e-04-3.7e-17i"
[1] "994 4.11494885432857e-04+4.7e-17i 149780 4.11487618905255e-04-3.7e-17i"
[1] "995 4.11504994606922e-04-3.9e-17i 149800 4.11487636368272e-04-3.7e-17i"
[1] "996 4.11507807864887e-04+1.7e-16i 149820 4.11487656620778e-04-3.7e-17i"
[1] "997 4.11507072061461e-04+4.58e-16i 149840 4.11487676094641e-04-3.7e-17i"
[1] "998 4.11501640003581e-04+2.08e-16i 149860 4.11487690086533e-04-3.6e-17i"
[1] "999 4.11488540757704e-04-5.3e-17i 149880 4.11487690938056e-04-3.6e-17i"
[1] "1000 4.1146528589172e-04-2.984e-15i 149900 4.1148766853301e-04-3.9e-17i"
```

The partial Euler Product based estimate after averaging above using truncation at $3N_1$ $Z(0.5 + I * 388858886) \approx 4.1148766853301e - 04 - 3.9e - 17i$ agrees to 8 decimal places with respect to the known Riemann-Siegel Z function value $Z(0.5 + I * 388858886) = 0.00041148914820069374095342320372253831362 + 9.442756329679734991E - 33 * I$

The above tabular results are also summarized in figure 3 showing the improvement in precision by using averaging and reducing bias using longer truncation lengths.

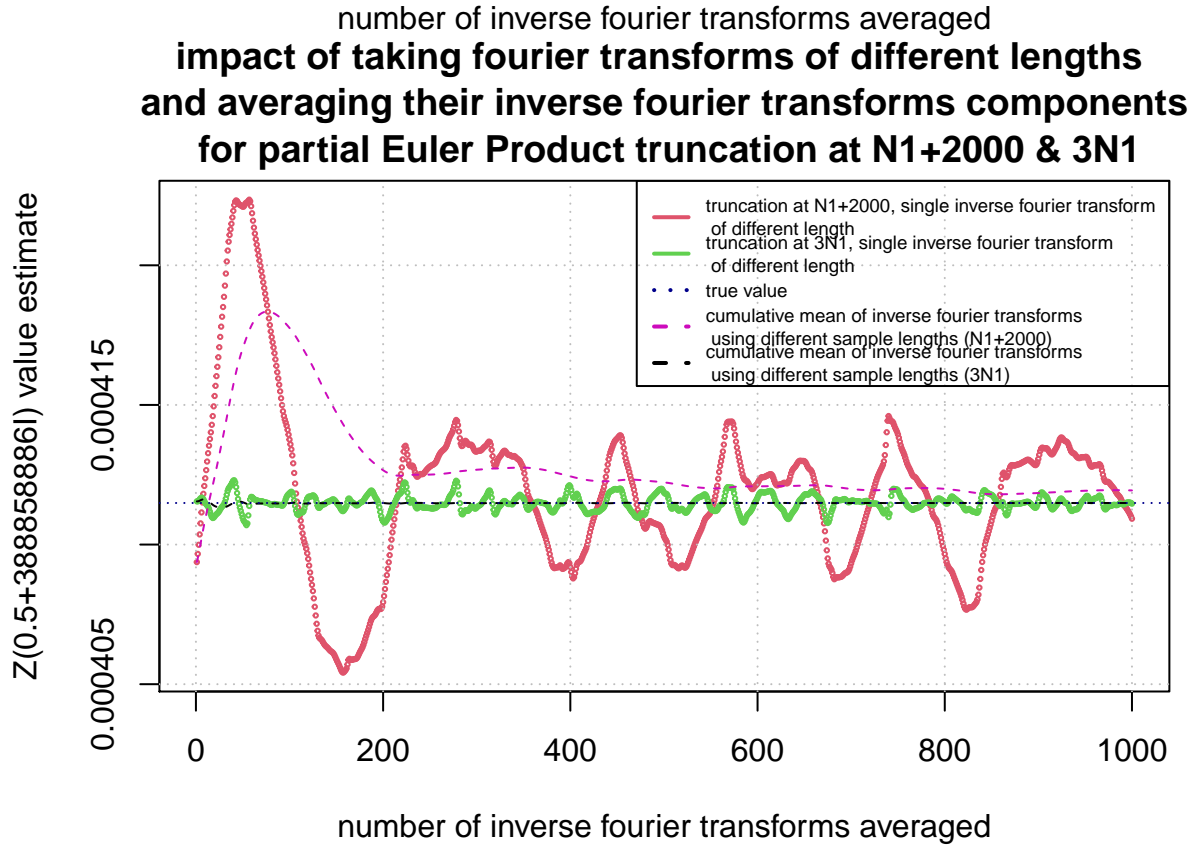
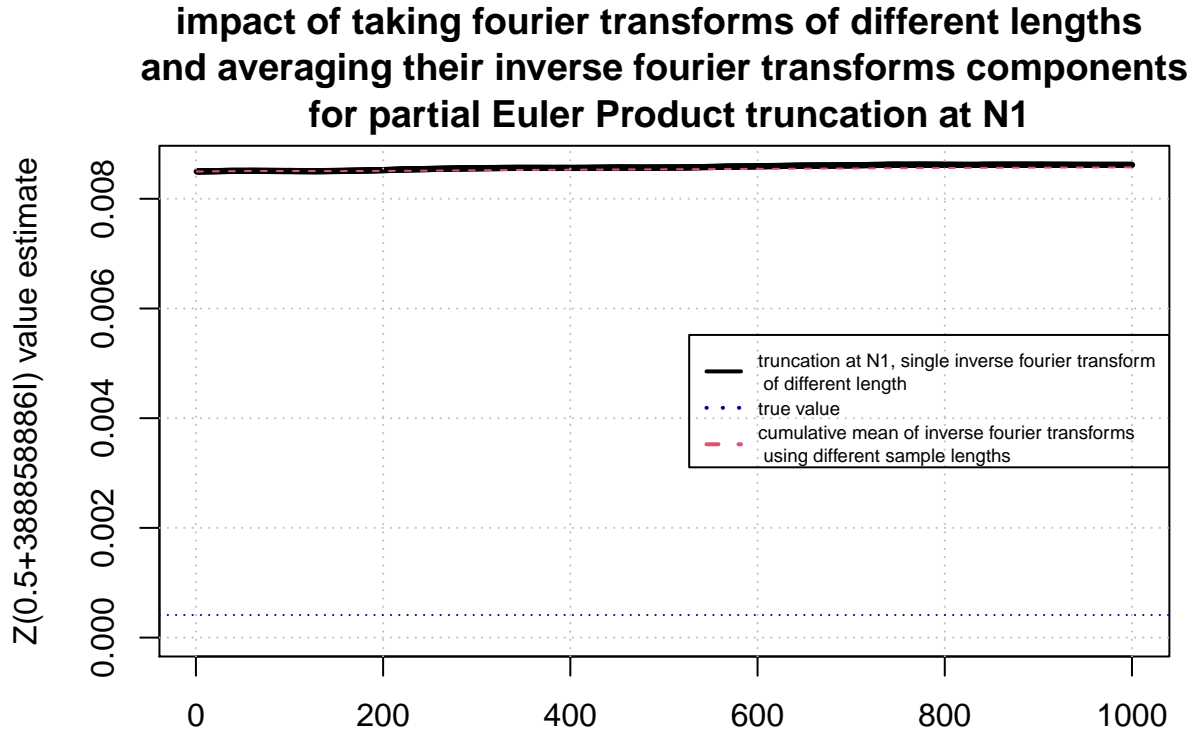


Figure 3: A comparison of the impact of averaging fourier transforms and inverse fourier transforms of different lengths of the partial Euler Product using three truncation lengths (top panel $N_1 = \sqrt{\frac{t}{2\pi}}$, bottom panel $N_1 + 2000$ and $3N_1$) for the Riemann-Siegel Z function approximation at $\sigma = 0.5 + I \cdot 388858886$.

The following example shows the benefit of analyzing data from a wider spectrum $t=388858886+(-7500,7500)$

example B; reference value - Riemann-Siegel Z function value at $s = 0.5 + I \cdot 388858886$

using fourier transform of first component of partial Euler product approximation of Riemann-Siegel Z function applying spectral filtering and phase conjugate reflection about DC component setting imaginary part of DC fourier component to zero for n real setting only the imaginary part of $(\text{ceiling}(n/2)+1)$ fourier component to zero in partial Euler product approximation

pari-gp [8] calculation using 128 tapered Dirichlet series truncation at N_1

```
dirichRS_S_sum128(0.5+I*388858886)*exp(I*vtheta(388858886))
```

```
time = 116 ms.
```

```
%31 = 0.00041148914820069374095342320372253831362 + 9.442756329679734991 E-33*I
```

approximation 4 - based on partial Euler Product truncation at $N_1 + 2000$

using much wider spectrum collected in the interval $t=388858886+(-7500,7500)$

maximum available sample $n=1,499,999$

below is the inverse fourier transform result for the Riemann-Siegel Z function at $s = 0.5 + I \cdot 388858886$ under 1000 iterations of fourier transforms of different sample lengths

```
[1] "index; single run estimate; sample length; cumulative average"
[1] "1 4.11466038283134e-04-5.8e-16i 1300100 4.11466038283134e-04-5.8e-16i"
[1] "2 4.11453528611139e-04-4.838e-15i 1300300 4.11459783447137e-04-2.709e-15i"
[1] "3 4.11433677848974e-04-5.05e-16i 1300500 4.11451081581082e-04-1.974e-15i"
[1] "4 4.11424717555921e-04+2.329e-15i 1300700 4.11444490574792e-04-8.99e-16i"
[1] "5 4.11423227942308e-04+3.583e-15i 1300900 4.11440238048295e-04-2e-18i"
[1] "6 4.11430182984948e-04-2.845e-15i 1301100 4.11438562204404e-04-4.76e-16i"
[1] "7 4.11439874335925e-04+1.234e-15i 1301300 4.11438749651764e-04-2.32e-16i"
[1] "8 4.11451171204889e-04-5.75e-16i 1301500 4.11440302345905e-04-2.75e-16i"
[1] "9 4.11475119378088e-04-2.784e-15i 1301700 4.11444170905036e-04-5.54e-16i"
[1] "10 4.11500703053298e-04+2.033e-15i 1301900 4.11449824119862e-04-2.95e-16i"
...
[1] "991 4.1151488055867e-04+1.237e-15i 1498100 4.11488807848297e-04-2.05e-16i"
[1] "992 4.11522091084896e-04-3.484e-15i 1498300 4.11488841399947e-04-2.08e-16i"
[1] "993 4.11527492831721e-04+2.036e-15i 1498500 4.11488880323846e-04-2.06e-16i"
[1] "994 4.115310211014e-04-9.54e-16i 1498700 4.11488922718994e-04-2.07e-16i"
[1] "995 4.11518603004167e-04-1.422e-15i 1498900 4.11488952548427e-04-2.08e-16i"
[1] "996 4.11511187298495e-04-3.66e-16i 1499100 4.11488974872473e-04-2.08e-16i"
[1] "997 4.11498875585709e-04+8.93e-16i 1499300 4.11488984802978e-04-2.07e-16i"
[1] "998 4.11482914140921e-04-7.7e-16i 1499500 4.1148897872015e-04-2.08e-16i"
[1] "999 4.11473488798251e-04+9.399e-15i 1499700 4.11488963214723e-04-1.98e-16i"
[1] "1000 4.11467236398466e-04+1.992e-15i 1499900 4.11488941487906e-04-1.96e-16i"
```

The partial Euler Product based approach analyzing a wider spectrum $t = 388858886 + (-7500, 7500)$ but with the same grid point spacing $\delta t = 0.01$ before (after) averaging above using truncation at $N_1 + 2000$ has the estimates $Z(0.5 + I \cdot 388858886) \approx 4.11466038283134e - 04 - 5.8e - 16i$ ($Z(0.5 + I \cdot 388858886) \approx 4.11488941487906e - 04 - 1.96e - 16i$) agrees to 7 (8) decimal places with respect to the known Riemann-Siegel Z function value $Z(0.5 + I \cdot 388858886) = 0.00041148914820069374095342320372253831362 + 9.442756329679734991E - 33 \cdot I$ showing the value in reducing the need for averaging by using a wider input spectrum.

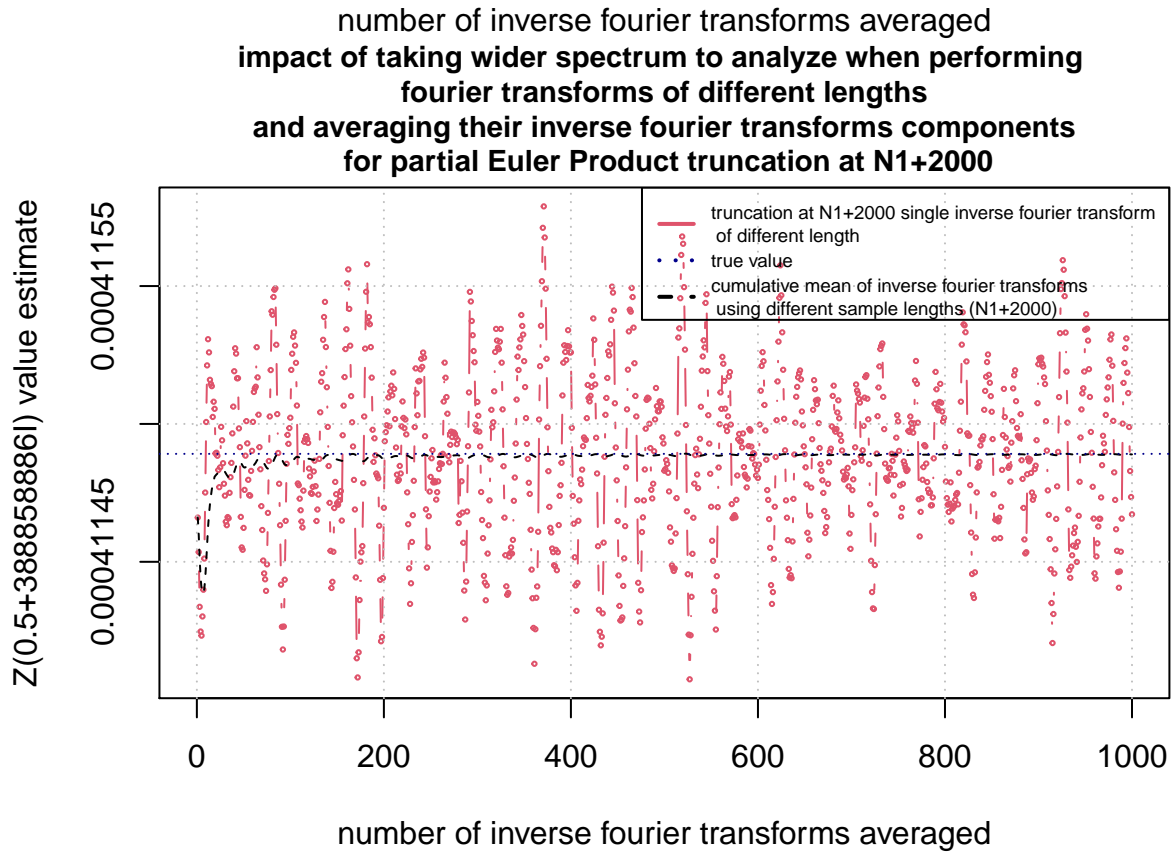
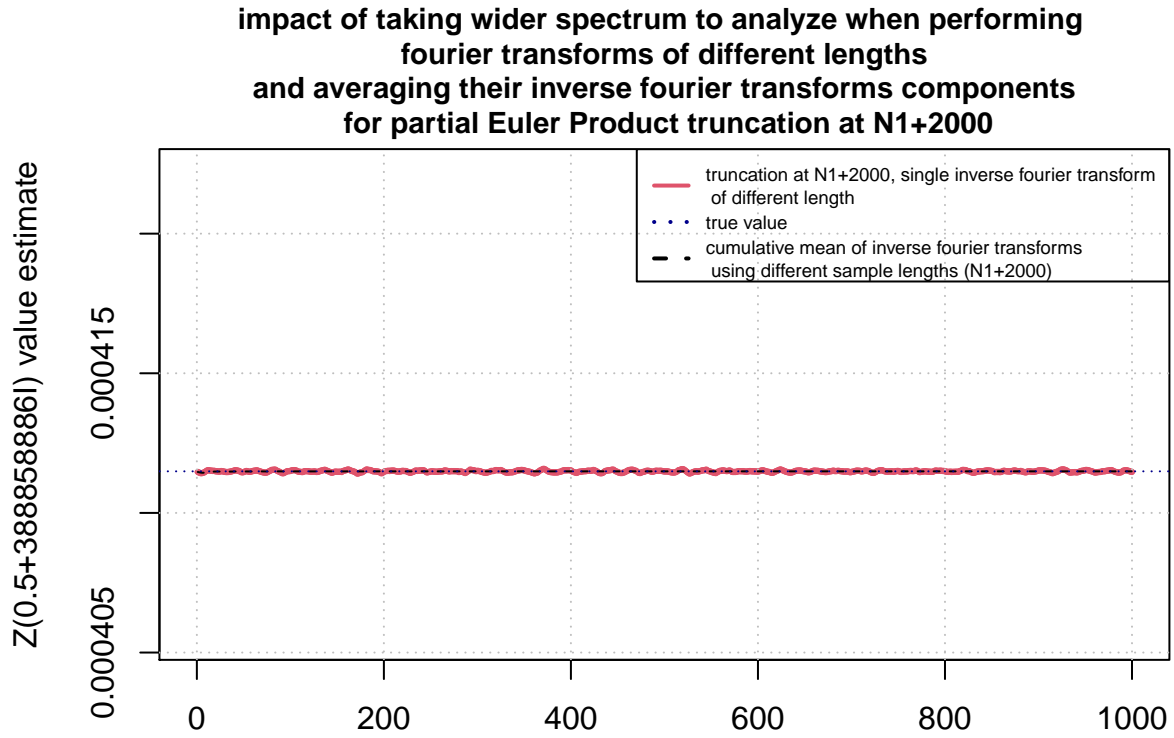


Figure 4: A comparison of the impact of averaging fourier transforms and inverse fourier transforms of different lengths of the partial Euler Product using truncation length $N_1 + 2000$ based on wider spectrum $t=388858886+(-7500,7500)$ for the Riemann-Siegel Z function approximation at $\sigma = 0.5 + I \cdot 388858886$. The scale in the top panel is the same as figure 3 indicating the wider spectrum can result in more accurate results for truncation length $N_1 + 2000$. The bottom panel shows the improvement in accuracy with averaging inverse fourier transforms of different length.

Figure 5 shows the errors in the fitted values of the spectrum grid ($\delta t = 0.01$) for example B in the region $t=(388858884, 388858888)$ in comparison to the true Riemann-Siegel Z function. The fitted values for the grid points (include averaging over the 1000 fourier analyses of different sample lengths) hence for $s = 0.5 + I * 388858886$ the error calculation is $\epsilon = \text{real}(4.11488941487906e - 04 - 1.96e - 16i) - \text{real}(0.00041148914820069374095342320372253831362 + 9.442756329679734991E - 33 * I) \approx -2.067128e - 10$.

Errors of fitted values of fourier grid points (dt=0.01 spacing) of partial Euler Product approximation using truncation at N_1+2000 using spectral filtering, phase conjugate reflection, two imputes and averaging

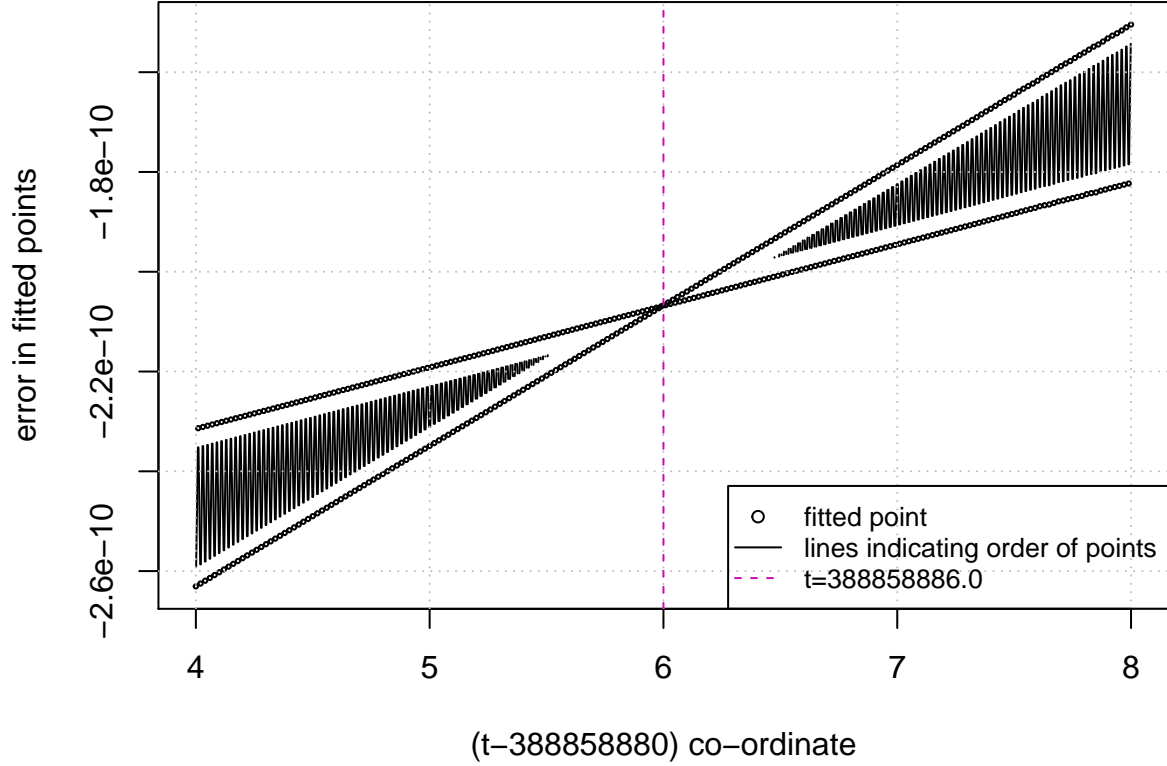


Figure 5: Errors in fitted values of inverse fourier transform approximation based on the partial Euler Product using truncation length $N_1 + 2000$ using spectral filtering, phase conjugate reflection, two imputed imaginary zeroes and averaging inverse fourier transforms of different lengths analyzing the wider spectrum $t=388858886+(-7500,7500)$ on the critical line around $\sigma = 0.5 + I \cdot 388858886$

It is important to note from a practical standpoint that

- what is meant by averaging the inverse fourier transforms of different length fourier samples is that (i) given the single input dataset with (time) domain $t=388858886+(-7500,7500)$ with grid size 0.01 which has 1499999 fourier components, (ii) different length fourier sample analysis involves taking samples $t=388858886+(-7499,7499)$, $t=388858886+(-7498,7498)$, $t=388858886+(-7497,7497)$, ..., $t=388858886+(-6499,6499)$ from the single input dataset and performing fourier analysis of the first component of equation (7) (but with truncation $N_1 + \Delta$ using spectral filtering, phase conjugate reflection, imputation of imaginary part zero for $\text{fft}[1]$, $\text{fft}[\lceil n/2 \rceil + 1]$ followed by calculating the inverse fourier transform and storing and/or averaging the results for the inverse fourier components common to all the different samples length (i.e. the smallest analyzed spectrum interval $t=388858886+(-6499,6499)$ where the results for the interval $t=388858886+(-2,2)$ has been presented in this paper). The common results are fitted points $388858886+(-6499, \dots, -2, -1.99, -1.98, \dots, -0.03, -0.02, -0.01, 0, 0.01, 0.02, 0.03, \dots, 6499)$.
- what appears to be happening with different sample sizes is that the spectral leakage/aliasing from high frequency components in the partial Euler product that are not contained in the Riemann-Siegel Z function or Riemann Zeta function differs in magnitude/sign and by averaging the impact of the spectral leakage/aliasing is greatly reduced.
- the differing fourier samples use sizes rounded to nearest tens, hundreds or thousands (depending on initial maximum available sample e.g. 149999, 1499999, 14999999) in order to avoid the **exceedingly long** fourier analysis computation times that occur with fourier sample sizes equal to large prime numbers.

Using spline interpolation to obtain preliminary estimates of the non-trivial zero positions

Since discrete fourier analysis only provides a explicit fit of the grid of input data points, spline interpolation between the fitted points of the inverse fourier transform can provide a preliminary estimate of other data points (t co-ordinate values) including zero crossings.

Figure 6 shows the predicted Riemann-Siegel Z function behaviour using spline interpolation of the averaged inverse fourier transform where the fourier analysis was based on an input grid size of $\delta t = 0.01$. It can be seen that the spline interpolation provides preliminary estimates of closely spaced non-trivial zeroes between $t=388858886.0022$ and $t=388858886.0024$ but the positions are not aligned with the known values [6,7].

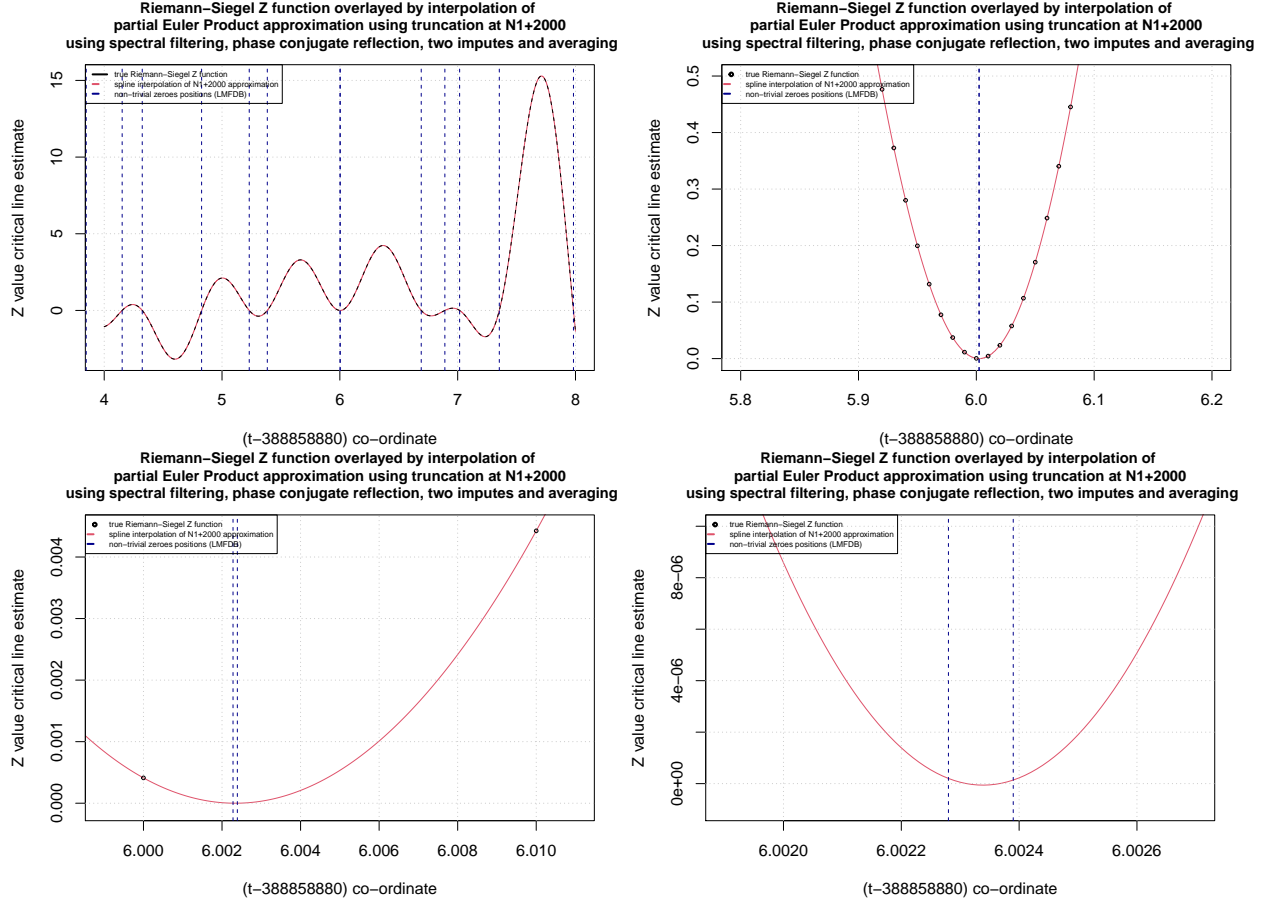


Figure 6: Using an input grid size of $\delta t = 0.01$. A comparison of the true Riemann-Siegel Z function and the inverse fourier transform approximation based on the partial Euler Product using truncation length $N_1 + 2000$ using spectral filtering, phase conjugate reflection, two imputed imaginary zeroes and averaging inverse fourier transforms of different lengths analyzing the on wider spectrum $t=388858886+(-7500,7500)$ on the critical line around $\sigma = 0.5 + I \cdot 388858886$. Each panel shows a progressively magnified closeup of the closely spaced zeroes at $t=388858886.0022851\dots$ and $t=388858886.0023936\dots$ [6,7].

Using a finer input grid $\delta t = 0.001$

Given the difference between preliminary estimates of the closely spaced Riemann-Siegel Z function non-trivial zeroes and their known values in figure 6. Spectral filtered partial Euler Product based approximation of the Riemann-Siegel Z function with grid size $\delta t = 0.001$ is also attempted.

example C;

approximation 5 - using spectrum collected with grid size $\delta t = 0.001$ in the interval $t=38858886+(-3832.622,3769.377)$ based on partial Euler Product truncation at $N_1 + 2000$

maximum available sample $n=7,602,060$

below is the inverse fourier transform result for the Riemann-Siegel Z function at $s = 0.5 + I \cdot 38858886$ under 100 iterations of fourier transforms of different sample lengths

```
[1] "index; single run estimate; sample length; cumulative average"
[1] "1 4.11362087990669e-04+1.468e-15i 7404000 4.11362087990669e-04+1.468e-15i"
[1] "2 4.1203224202535e-04+2.968e-15i 7406000 4.1169716500801e-04+2.218e-15i"
[1] "3 4.11530613334881e-04-2.686e-15i 7408000 4.11641647783633e-04+5.83e-16i"
[1] "4 4.08697304819609e-04+7.37e-16i 7410000 4.10905562042627e-04+6.22e-16i"
[1] "5 4.10296247345262e-04+2.262e-15i 7412000 4.10783699103154e-04+9.5e-16i"
[1] "6 4.10956890543605e-04+1.2899e-14i 7414000 4.10812564343229e-04+2.941e-15i"
[1] "7 4.11330379679623e-04-1.6023e-14i 7416000 4.10886537962714e-04+2.32e-16i"
[1] "8 4.11711510463301e-04+6.75e-15i 7418000 4.10989659525287e-04+1.047e-15i"
[1] "9 4.12292651175126e-04+1.0295e-14i 7420000 4.11134436375269e-04+2.074e-15i"
[1] "10 4.12407567449154e-04+1.7412e-14i 7422000 4.11261749482658e-04+3.608e-15i"
...
[1] "91 4.11255089089398e-04+2.206e-15i 7584000 4.11530814797245e-04+1.387e-15i"
[1] "92 4.12629367637724e-04-5.9258e-14i 7586000 4.1154275558899e-04+7.28e-16i"
[1] "93 4.10343570399683e-04-4.684e-15i 7588000 4.11529861124589e-04+6.7e-16i"
[1] "94 4.10850329210734e-04-2.9e-17i 7590000 4.11522632061675e-04+6.63e-16i"
[1] "95 4.11747187646636e-04+1.641e-15i 7592000 4.11524995804675e-04+6.73e-16i"
[1] "96 4.11188429188644e-04-4.4185e-14i 7594000 4.11521489902425e-04+2.06e-16i"
[1] "97 4.12052049816024e-04-7.425e-15i 7596000 4.11526959592255e-04+1.27e-16i"
[1] "98 4.11607681569761e-04-2.329e-15i 7598000 4.11527783285903e-04+1.02e-16i"
[1] "99 4.12031416315095e-04+2.061e-15i 7600000 4.11532870488219e-04+1.22e-16i"
[1] "100 4.10751669041205e-04-7.2e-17i 7602000 4.11525058473748e-04+1.2e-16i"
```

It can be seen that the single sample results of example C are noisier than example B which is related to the use of a smaller grid size but there are now fitted grid points available for 38858886.001, 38858886.002, 38858886.003, 38858886.004 which will be useful for spline interpolation between 38858886.002 and 38858886.003. Figure 7 then presents the results of the fitted points of this finer input grid size of $\delta t = 0.001$ calculation and it can be seen that the spline interpolation now provides preliminary estimates of closely spaced non-trivial zeroes well aligned with the known values [6,7].

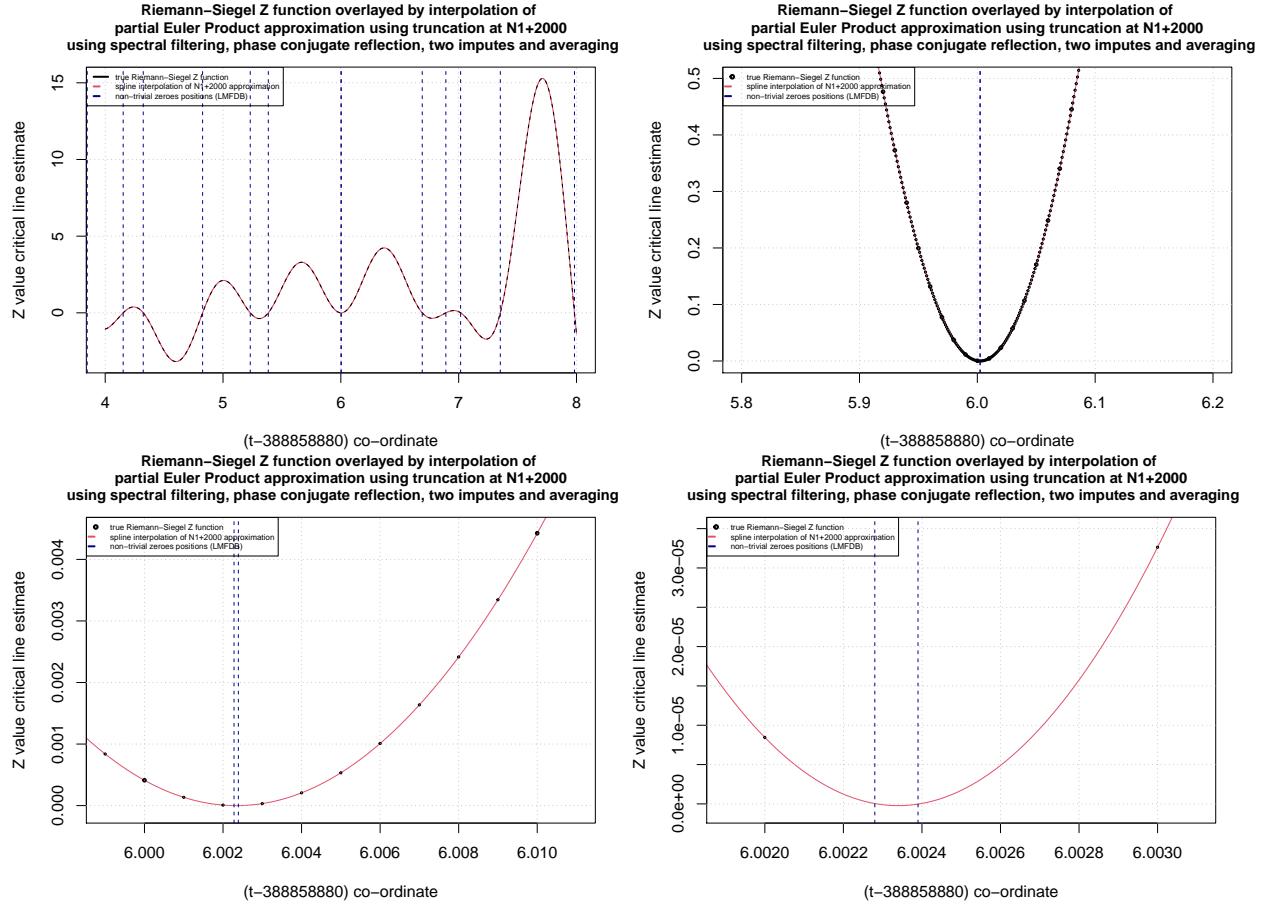


Figure 7: Using an input grid size of $\delta t = 0.001$. A comparison of the true Riemann-Siegel Z function and the inverse fourier transform approximation based on the partial Euler Product using truncation length $N_1 + 2000$ using spectral filtering, phase conjugate reflection, two imputed imaginary zeroes and averaging inverse fourier transforms of different lengths analyzing the wider spectrum $t=38858886+(-3832.622,3769.377)$ on the critical line around $\sigma = 0.5 + I \cdot 38858886$. Each panel shows a progressively magnified closeup of the closely spaced zeroes at $t=38858886.0022851\dots$ and $t=38858886.0023936\dots$ [6,7].

Finally approximation 6 which uses a wider input spectrum $t=388858886+(-7500,7500)$ for fourier analysis than approximation 5 ($t=388858886+(-3832.622,3769.377)$) has (i) lower noise closer to example B's behaviour in its cumulative averaging results below and (ii) continues to display in Figure 7 that the spline interpolation preliminary estimates (based on $\delta t = 0.001$ grid) of zero crossings remain well aligned with the known non-trivial zeroes values [6,7].

approximation 6 - using wider spectrum collected with grid size $\delta t = 0.001$ in the interval $t=388858886+(-7500,7500)$ based on partial Euler Product truncation at $N_1 + 2000$

maximum available sample $n=15,000,001$

below is the inverse fourier transform result for the Riemann-Siegel Z function at $s = 0.5 + I \cdot 388858886$ under 100 iterations of fourier transforms of different sample lengths

```
[1] "index; single run estimate; sample length; cumulative average"
[1] "1 4.11523313832241e-04+7.747e-15i 14802000 4.11523313832241e-04+7.747e-15i"
[1] "2 4.11523361236886e-04-5.037e-15i 14804000 4.11523337534563e-04+1.355e-15i"
[1] "3 4.11523684025954e-04-2.52e-16i 14806000 4.11523453031694e-04+8.19e-16i"
[1] "4 4.11517358095215e-04+1.171e-15i 14808000 4.11521929297574e-04+9.07e-16i"
[1] "5 4.11518825424092e-04-8.59e-16i 14810000 4.11521308522877e-04+5.54e-16i"
[1] "6 4.11515815020734e-04+2.6e-17i 14812000 4.11520392939187e-04+4.66e-16i"
[1] "7 4.11508480722641e-04+9.3e-17i 14814000 4.11518691193966e-04+4.13e-16i"
[1] "8 4.11496329588964e-04+1.232e-15i 14816000 4.11515895993341e-04+5.15e-16i"
[1] "9 4.11482121378464e-04-3.48e-16i 14818000 4.11512143258355e-04+4.19e-16i"
[1] "10 4.11471496624231e-04-2.96e-16i 14820000 4.11508078594942e-04+3.48e-16i"
...
[1] "91 4.11519335612193e-04+3.166e-15i 14982000 4.11488756582388e-04+2.8e-16i"
[1] "92 4.11525330814178e-04-9.941e-15i 14984000 4.11489154128386e-04+1.69e-16i"
[1] "93 4.11529577880114e-04-1.06e-15i 14986000 4.11489588792383e-04+1.56e-16i"
[1] "94 4.11527478420714e-04+5.91e-16i 14988000 4.11489991873536e-04+1.6e-16i"
[1] "95 4.11516275820512e-04+8.3e-17i 14990000 4.11490268546662e-04+1.6e-16i"
[1] "96 4.11506597387029e-04-8.63e-16i 14992000 4.11490438638749e-04+1.49e-16i"
[1] "97 4.11489778760425e-04-1.059e-15i 14994000 4.1149043183588e-04+1.37e-16i"
[1] "98 4.11478113876259e-04+5e-18i 14996000 4.11490306142414e-04+1.35e-16i"
[1] "99 4.11469942953073e-04+1.4821e-14i 14998000 4.11490100453633e-04+2.84e-16i"
[1] "100 4.11463989375082e-04+2.514e-15i 15000000 4.11489839342847e-04+3.06e-16i"
```

where the reference value for comparison of the Riemann-Siegel Z function at $s = 0.5 + I \cdot 388858886.0$ is $Z(0.5 + I \cdot 388858886) = 0.00041148914820069374095342320372253831362 + 9.442756329679734991E - 33 * I$

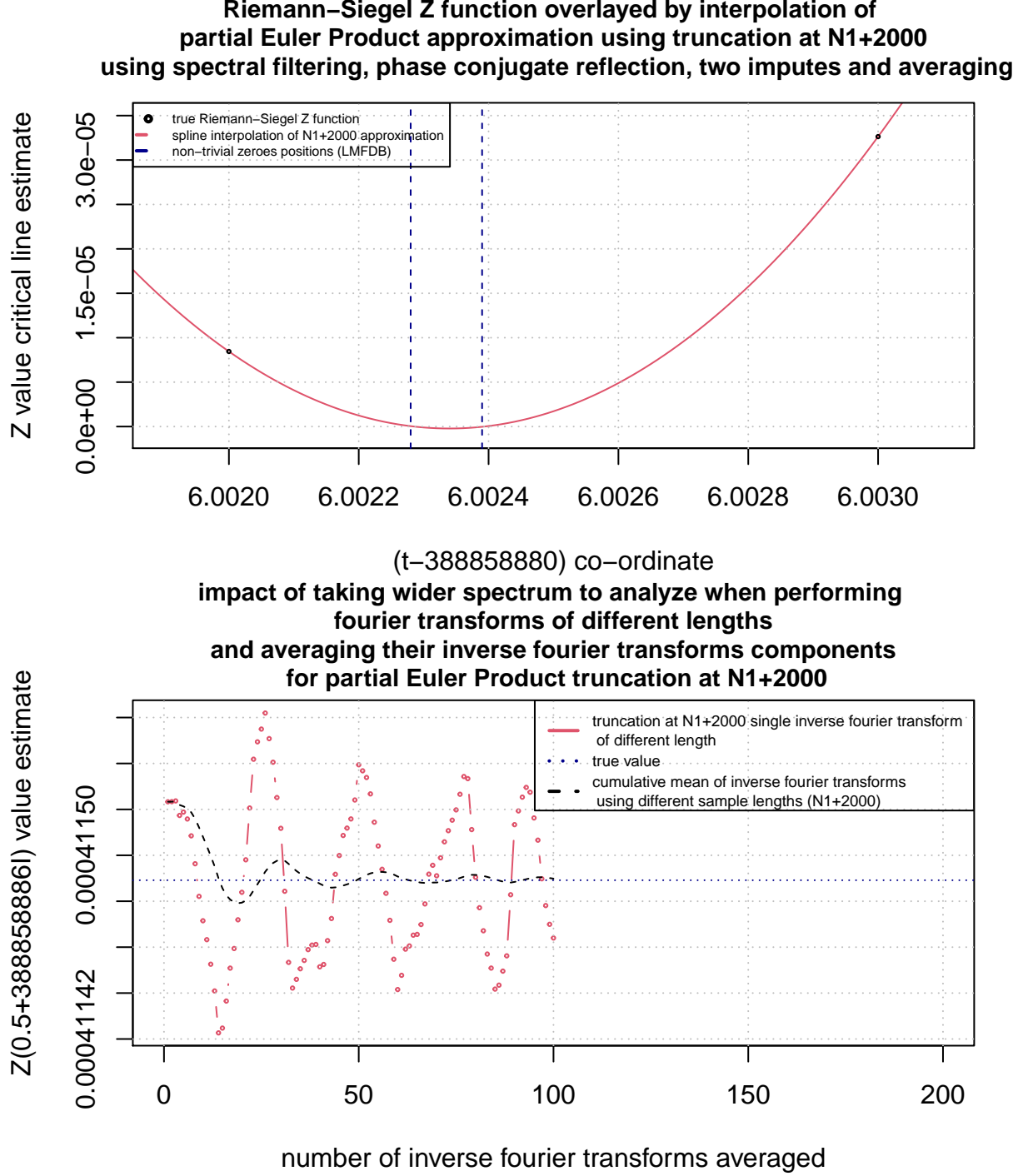


Figure 8: Using an input grid size of $\delta t = 0.001$. A comparison of the true Riemann–Siegel Z function and (i) the inverse fourier transform approximation at $t=388858886.002, 388858886.003$ (circle) based on the partial Euler Product using truncation length $N_1 + 2000$ using spectral filtering, phase conjugate reflection, two imputed imaginary zeroes and averaging inverse fourier transforms of different lengths analyzing the on wider spectrum $t=388858886+(-7500,7500)$ on the critical line around $\sigma = 0.5 + I \cdot 388858886$ and (ii) spline interpolation (red line) fitting the whole grid of inverse fourier transform approximations with grid spacing $\delta t = 0.001$. The top panel shows a closeup of the closely spaced zeroes at $t=388858886.0022851\dots$ and $t=388858886.0023936\dots$ [6,7] and the spline interpolation preliminary estimates of the zero crossings. The bottom panel shows the improvement in the inverse fourier transformation approximation accuracy by using averaging of inverse fourier transforms of different length.

Conclusions

The above steps of spectral filtering, phase conjugate reflection, imputation of zero imaginary parts for two fourier components, using truncation lengths of $N_1 + \Delta$ and averaging of the inverse fourier transform results under different spectrum widths leads to a robust partial Euler Product based approximations of the Riemann-Siegel function useful for examining closely separated Riemann Zeta function non-trivial zeroes (away from the real axis). In the above fourier analysis processing, spectral leakage from high frequency components present in the partial Euler Product but not present in the Riemann Zeta function is greatly suppressed (where the choice of input grid size for fourier analysis, the maximum width of the input spectrum, the truncation length $N_1 + \Delta$ and the number of different length fourier samples to be averaged all influence the robustness for examining closely spaced Riemann-Siegel Z function non-trivial zeroes).

References

1. Edwards, H.M. (1974). Riemann's zeta function. Pure and Applied Mathematics 58. New York-London: Academic Press. ISBN 0-12-232750-0. Zbl 0315.10035.
2. Riemann, Bernhard (1859). "Über die Anzahl der Primzahlen unter einer gegebenen Grösse". Monatsberichte der Berliner Akademie.. In *Gesammelte Werke*, Teubner, Leipzig (1892), Reprinted by Dover, New York (1953).
3. Titchmarsh, E.C. (1986) *The Theory of the Riemann Zeta Function*. 2nd Revised (Heath-Brown, D.R.) Edition, Oxford University Press, Oxford.
4. Berry, M. V. "The Riemann-Siegel Expansion for the Zeta Function: High Orders and Remainders." *Proc. Roy. Soc. London A* 450, 439-462, 1995.
5. Martin, J.P.D. "A useful approximation of the Riemann Zeta function away from the real axis using spectral filtering of the partial Euler product" (2025) <http://dx.doi.org/10.6084/m9.figshare.28528652>
6. van de Lune J., te Riele H.J.J. and Winter D.T. (1986) "On the Zeros of the Riemann Zeta function in the Critical Strip. IV" *Mathematics of Computation*, Volume 46, Pages 667-681
7. The LMFDB Collaboration, The L-functions and Modular Forms Database, <http://www.lmfdb.org>
8. The PARI-Group, PARI/GP version 2.12.0, Univ. Bordeaux, 2018, <http://pari.math.u-bordeaux.fr/>.
9. R Core Team (2017). R: A language and environment for statistical computing. R Foundation for Statistical Computing, Vienna, Austria. <https://www.R-project.org/>.
10. RStudio Team (2015). RStudio: Integrated Development for R. RStudio, Inc., Boston, MA URL <http://www.rstudio.com/>.
11. Taboga, M (2021). "Discrete Fourier transform of a real signal", *Lectures on matrix algebra*. <https://www.statlect.com/matrix-algebra/discrete-Fourier-transform-of-a-real-signal>.